

A Bayesian analysis of the primordial power spectrum

M. Bridges,^{1*} A.N. Lasenby,¹ M.P. Hobson¹

¹*Astrophysics Group, Cavendish Laboratory, Madingley Road, Cambridge CB3 0HE, UK*

Accepted —. Received —; in original form 11 March 2019

ABSTRACT

We present a Bayesian analysis of large-scale structure and cosmic microwave background data to constrain the form of the primordial power spectrum. We have extended the usual presumption of a scale invariant spectrum to include: (i) a running spectral index; (ii) a broken spectrum arising perhaps from an interruption of the potential driving inflation; (iii) a large scale cutoff in power as the first year WMAP results appear to indicate; (iv) a reconstruction of the spectrum in eight bins in wavenumber; and (v) a spectrum resulting from a cosmological model proposed by Lasenby & Doran, which naturally exhibits an exponential drop in power on very large scales. The result of our complete Bayesian analysis includes not only the posterior probability distribution from which parameter estimates are inferred but also the Bayesian evidence. This evidence value is greater for a model with fewer parameters unless a more complicated model provides a significantly better fit to the data, thus allowing a powerful method of model selection. We find that those models exhibiting any form of cutoff in power on large scales consistently produce higher evidences than either the Harrison-Zel'dovich or single spectral index spectra. In particular, within the best-fit concordance cosmology, we find the Lasenby & Doran spectrum to show significantly larger evidence as compared to the other models.

Key words: cosmological parameters – cosmology:observations – cosmology:theory – cosmic microwave background – large scale structure

1 INTRODUCTION

Recent cosmological surveys of the cosmic microwave background (CMB), in particular observations by the Wilkinson Microwave Anisotropy Probe (WMAP), and large scale structure data, such as from the two degree field galaxy redshift survey (2dFGRS), have provided a unique tool in constraining the structure and contents of the Universe (Spergel et al. 2003; Rebolo et al. 2004). One of the most exciting results to emerge from these analyses is possible structure in the primordial power spectrum, features in which can be used to constrain early Universe physics, including inflationary models.

The simplest model of inflationary perturbation generation involves a single, slowly rolling inflaton field producing a nearly scale-invariant spectrum, although even this is only true in the limit of an infinitely slow roll with infinite Hubble expansion damping (Dodelson 2002). More generally, phase transitions from force unification in the early Universe (Barriga et al. 2001), multiple field inflation, hybrid inflation (Linde 1983) and other models (Adams, Ross & Sarkar 1997; Wang 1994) all produce features in the primordial

spectrum. It should also be noted that a scale-invariant spectrum does *not* uniquely identify inflation as the source of density perturbations, but a spectrum containing specific features *would* be indicative of a specific model of inflation. Hence the study of the form of the spectrum is crucial in analysis of future data.

Generalisations of the shape of the primordial spectrum have been attempted on various physical and observational grounds to construct an *a priori* parameterisation (e.g. Bridle et al. 2003), while others have attempted to reconstruct an unknown spectrum directly from the data (Wang 1994; Bridle et al. 2003; Tocchini-Valentini, Douspis & Silk 2005; Hannestad 2004). In this paper we will mostly employ the latter method, following closely the Bridle et al. analysis despite the obvious disadvantage of weakening constraints on remaining cosmological parameters and the creation of further degeneracies by the inclusion of more primordial parameters. One may, however employ a fully Bayesian extension of the Markov-Chain Monte Carlo (MCMC) method (see Sec. 2.1) to select the most appropriate model according to its Bayesian evidence (see Slosar et al. 2003; Beltran et al. 2005; Trotta 2005 and most recently Mukherjee, Parkinson & Liddle 2005). This method favours simple models with fewer parameters over a

* E-mail: m.bridges@mrao.cam.ac.uk

more elaborate model, unless the latter can provide a substantially better fit to the data.

Using a parameterised spectrum requires constraining any analysis to a small sample of the huge number of possibilities, some of which have been outlined above. Observational features can refine the choice, for example the apparently low power observed in the first three CMB multipoles by WMAP. Although some authors (Efstathiou 2003a) have suggested that these results are not statistically significant, in our analysis these data will always prefer a model with low power on these scales. We also test a broken spectrum caused perhaps by a double field inflationary potential or momentary pauses in the slow roll of the inflaton (Barriga et al. 2001). Lasenby & Doran (2005) arrived at a spectrum naturally incorporating an exponential fall off in power on large scales by considering evolution of closed Universes out of a big bang singularity and with a novel boundary condition that restricts the total conformal time available in the Universe. The fact that this model features the type of cutoff that has been suggested on phenomenological grounds from the data (Efstathiou 2003b) make it an intriguing possibility.

2 MODEL SELECTION FRAMEWORK

2.1 Markov Chain Monte Carlo sampling

A Bayesian analysis provides a coherent approach to estimating the values of the parameters, Θ , and their errors and a method for determining which model, M , best describes the data, \mathbf{D} . Bayes theorem states that

$$P(\Theta|\mathbf{D}, M) = \frac{P(\mathbf{D}|\Theta, M)P(\Theta|M)}{P(\mathbf{D}|M)}, \quad (1)$$

where $P(\Theta|\mathbf{D}, M)$ is the posterior, $P(\mathbf{D}|\Theta, M)$ the likelihood, $P(\Theta|M)$ the prior, $P(\mathbf{D}|M)$ the Bayesian evidence. Conventionally, the result of a Bayesian parameter estimation is the posterior probability distribution given by the product of the likelihood and prior. In addition however, the posterior distribution may be used to evaluate the Bayesian evidence for the model under consideration.

We will employ a MCMC sampling procedure to explore the posterior distribution using an adapted version of the *cosmoMC* package (Lewis & Bridle 2002) with four CMB datasets; WMAP (Verde et al. 2003; Hinshaw et al. 2003; Kogut et al. 2003), ACBAR (Kuo et al. 2004) the latest VSA results (Dickinson et al. 2004) and CBI (Readhead et al. 2004). We also include the 2dF Galaxy Redshift Survey (Percival et al. 2001) and the Sloan Digital Sky Survey (Abazajian et al. 2003). In addition to the primordial spectrum parameters, we parameterise each model using the following five cosmological parameters; the physical baryon density $\Omega_b h^2$; the physical cold dark matter density $\Omega_c h^2$; the total energy density Ω_0 (parameterised as $\Omega_k = 1 - \Omega_0$); the Hubble parameter h ($H_0 = h \times 100 \text{ km s}^{-1}$) and the redshift of re-ionisation z_{re} .

2.2 Bayesian evidence and simulated annealing

The Bayesian evidence can be defined as the average likelihood over the entire parameter space of the model:

$$\int P(\mathbf{D}|\Theta, M)P(\Theta)d^N\Theta. \quad (2)$$

In general models with fewer parameters and hence small parameter spaces will have larger evidences. Naively one could evaluate the evidence by sampling from the posterior distribution function randomly covering the entire parameter space and simply find the average likelihood value. In practise however the value of the likelihood at its maximum is typically many orders of magnitude larger than that at any extremes of the space and so very many samples would need to be taken away from the peak in order for their inclusion to make any appreciable difference. To overcome this one can use the numerical method of simulated annealing, also known as thermodynamic integration, to slowly increase the height of the peak in the likelihood relative to the surrounding background value. Using a random sampling of the space, such as MCMC, one can ensure that all of the parameter space, not just the area around the peak likelihood is explored.

Using such an annealing schedule we draw samples from $P(\mathbf{D}|\Theta, M)^\lambda P(\Theta|M)$ where λ is the inverse temperature and is raised from ≈ 0 to 1. One can then define the evidence as a function of λ as

$$E(\lambda) = \int P(\mathbf{D}|\Theta, M)^\lambda P(\Theta|M)d^N\Theta. \quad (3)$$

We require that the priors be normalised to unity over the parameter space considered thus $E(\lambda = 0) = 1$ and we will also find it computationally simpler to work in the natural logarithm of evidences, therefore:

$$\begin{aligned} \ln E(\lambda) &= \ln E(0) + \int_0^1 \frac{d \ln E(\lambda)}{d\lambda} d\lambda \\ &= \int_0^1 \frac{d \ln E(\lambda)}{d\lambda} d\lambda \\ &= \int_0^1 \frac{1}{E} \frac{dE(\lambda)}{d\lambda} d\lambda. \end{aligned}$$

Performing the derivative of $E(\lambda)$ gives

$$\ln E(\lambda) = \int_0^1 \frac{\int P(\mathbf{D}|\Theta, M)^\lambda \ln P(\mathbf{D}|\Theta, M)P(\Theta|M)d^N\Theta}{\int P(\mathbf{D}|\Theta, M)^\lambda P(\Theta|M)d^N\Theta} d\lambda. \quad (4)$$

This gives the expectation value of $\ln P(\mathbf{D}|\Theta, M)$ over the parameter space defined by the extent of the priors. Thus we can simply sum over these values at each step $\Delta\lambda$ in the annealing schedule and divide by the total number of samples to find the log evidence value

$$\ln E(\lambda) \approx \frac{1}{N_\lambda} \sum_{i=1}^{N_\lambda} \ln P(\mathbf{D}|\Theta, M)_i. \quad (5)$$

The evaluation of this integral was performed using a reverse annealing schedule (as set out in Beltran et al. (2005)) where λ is lowered from 1 to 0 once the Markov chain has found its stationary point through a period of normal burn-in, which typically takes < 500 samples. The number of annealing steps N is not a chosen constant but is instead determined by the stopping criterion that the final log evidence value would not change by more than a given threshold (empirically set to 0.001). Accordingly λ at each step is given as:

$$\lambda(N) = (1 - \epsilon)^N. \quad (6)$$

where ϵ is a user defined parameter of order 5×10^{-5} . With this method log evidence values varying to within only one unit were successfully obtained from independent chains. The total number of sampler calls made during the evidence burn in was ≈ 3000 deliberately large to ensure the chain was at a stationary point. During the reverse annealing schedule typically ≈ 15000 calls were made.

3 PRIMORDIAL POWER SPECTRUM PARAMETERISATION

The correlation function ξ over a range r of a density field, such as the matter density field in the Universe is defined as the product of the density contrast at two separate points, \mathbf{x} and $\mathbf{x} + \mathbf{r}$

$$\xi(r) \equiv \langle \delta(\mathbf{x})\delta(\mathbf{x} + \mathbf{r}) \rangle. \quad (7)$$

The power spectrum $P(k)$ is simply the inverse Fourier transform of the correlation function or the ensemble average power:

$$P(k) \equiv \langle |\delta_k|^2 \rangle. \quad (8)$$

The basic inflationary paradigm inflates quantum zero-point oscillations of the inflaton to macroscopic scales, providing a source of density fluctuations which would then evolve via gravitational collapse to form the observed large scale structure today. The power spectrum of these primordial fluctuations can then provide unique constraints on the dynamics of the inflationary epoch. The homogeneity of the Universe on large scales suggests the simplest spectrum and most obvious first candidate is scale invariant. This intuition is confirmed by the results of slow-roll inflation, predicting the slightly sloped power law spectrum

$$P(k) = Ak^{n-1}. \quad (9)$$

where $|n - 1| \ll 1$. It can be shown that the Fourier components δ_k are uncorrelated and have random phases meaning the power spectrum encodes all of the stochastic properties of the density field.

3.1 Harrison-Zel'dovich and Power-Law Parameterisations

The simplest scale invariant power spectrum can be parameterised with one free parameter, an amplitude; A_s as:

$$P(k) = A_s, \quad (10)$$

This is known as the Harrison-Zel'dovich (H-Z) spectrum. Slow roll inflationary scenarios would be expected to imprint a slight slope, leading to the familiar power law form characterised by a spectral index n_s (see Eqn. 9) A link between n_s and the potential driving inflation is well established (Lyth and Riotto 1998) but the spectrum is only an exact power law for an exponential inflationary potential, so in general the spectral index should be some function of scale $n(k)$. Therefore we can also characterise the form of the spectrum as

$$P(k) = A_s \left(\frac{k}{k_0} \right)^{n-1+(1/2)\ln(k/k_0)(dn/d\ln k + \dots)}. \quad (11)$$

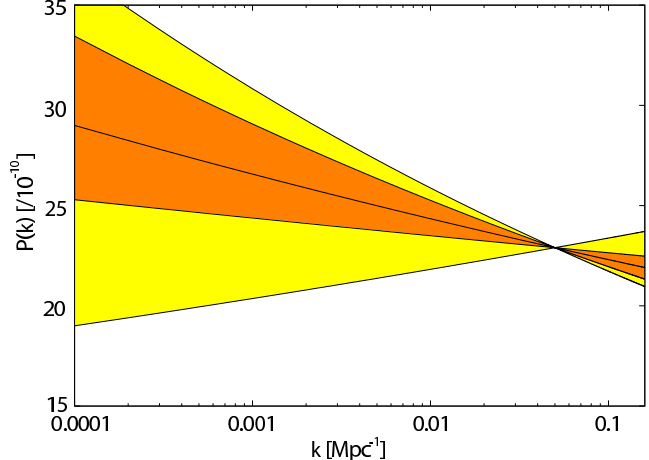


Figure 1. Best fit single spectral index power law spectrum with 1σ and 2σ errors (shown with shaded areas). [Note that, for clarity, the error in A_s is not shown]

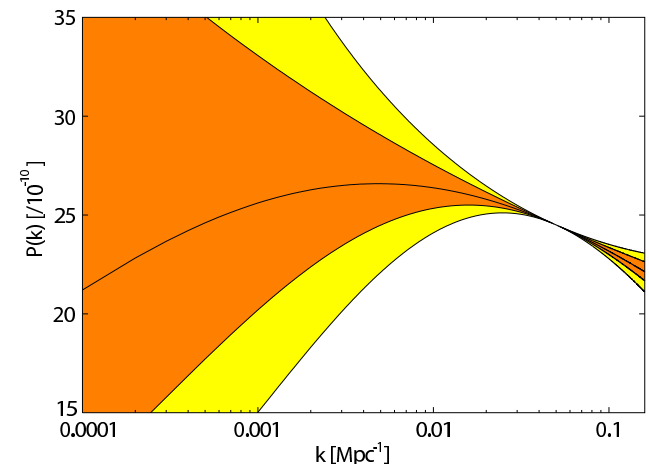


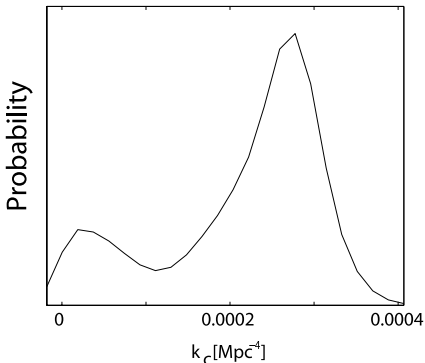
Figure 2. Best fit running spectral index power law spectrum with 1σ and 2σ errors (shown with shaded areas). [Note that, for clarity, the errors in A_s and n_s are not shown]

where $dn/d\ln k$ is the running parameter n_{run} . For most standard models we would expect $n_{run} \approx 0$. The entire spectrum pivots about a scale k_0 which is also the position in k -space at which the amplitude is set. In keeping with previous studies we have set this scale to 0.05 Mpc^{-1} .

The complete parameter estimates of our analysis using the data described above are shown in Table 1. The inclusion of the possibility of a non-flat geometry lowers the value of h considerably, a point to which we will return in Sec. 3.5. We find a best-fit single index spectrum (see Fig. 1) that, despite the inclusion of more recent data and extension to non-flat geometries, does not differ appreciably from the best-fit index found by Spergel et al. (2003). The inclusion of a running index (see Fig. 2) weakens the constraint slightly to 0.93 ± 0.05 . To 1σ level the constraint on n_{run} provides only slight evidence for a dependence of n_s on k .

Table 1. MCMC parameter constraints for H-Z, single index and running index parameterisations (mean $\pm 1\sigma$ errors)

Parameter	H-Z	Single Index	Running Index	Priors
n_s	-	0.96 ± 0.02	0.93 ± 0.05	[0.5,1.5]
n_{run}	-	-	-0.034 ± 0.032	[-0.15,0.15]
$A_s (\times 10^{-8})$	27.1 ± 1.1	22.6 ± 1.1	24.9 ± 1.2	[14.9,54.6]
$\Omega_b h^2$	0.0240 ± 0.0006	0.0229 ± 0.0009	0.0225 ± 0.0012	[0.005,0.1]
$\Omega_c h^2$	0.116 ± 0.009	0.118 ± 0.008	0.125 ± 0.012	[0.01,0.99]
Ω_k	$-0.026^{+0.018}_{-0.019}$	$-0.024^{+0.018}_{-0.019}$	$-0.022^{+0.020}_{-0.019}$	[-0.25,0.25]
h	$0.63^{+0.05}_{-0.06}$	0.61 ± 0.05	0.61 ± 0.05	[0.4,1]
z_{re}	19.0 ± 2.6	13.4 ± 4.2	16.4 ± 5.5	[4,30]

**Figure 3.** Marginalised histogram of the cutoff in power on large scales

3.2 Large Scale Cutoff

WMAP observations have pointed to lower than expected power on large scales. Although the statistical significance of these data points have been questioned (Efstathiou 2003b), currently models with a cutoff in power should be preferred. We did not attempt to model the form of the spectrum near the cutoff, instead parameterising the scale at which the power drops to zero, k_c , with a prior of $[0.0, 0.0006]$ Mpc $^{-1}$:

$$P(k) = \begin{cases} 0, & k < k_c \\ A_s \left(\frac{k}{k_0}\right)^{n-1}, & k \geq k_c \end{cases} \quad (12)$$

It is worth pointing out however that inherent cosmic variance limitations at this scale would make constraints of any form difficult to obtain.

On small scales this spectrum behaves just as the single index power law and so constraints on the cosmological parameters remain essentially unchanged. As shown in Fig. 3, a cutoff is preferred (see Fig.3) but the single index model is still not ruled out, illustrated by the non zero value of the likelihood function at $k_c = 0$. The likelihood function peaks at a cutoff scale of 2.7×10^{-4} Mpc $^{-1}$ and drops off markedly thereafter towards higher k_c . This figure reproduces well the results of Bridle et al. (2003) and despite a different mathematical form for the cutoff gives a similar likelihood distribution to Niarchou et al. (2004).

3.3 Broken Power Spectrum

Rapid cooling of the Universe during inflation can result in spontaneous symmetry breaking phase transitions which

could interrupt the potential driving inflation leading to one or more sudden departures in scale invariance lasting $\approx 1e$ fold (Barreira et al. 2001). When this occurs, the mass of the inflaton field changes suddenly, thus interrupting inflation. Although predicting the form of this interruption is not trivial, it is clear we should observe a drop in power, i.e. a break in the primordial power spectrum, after which the spectrum should return to scale invariance. We will assume the spectrum has the general form

$$P(k) = \begin{cases} A, & k \leq k_s \\ Ck^{\alpha-1}, & k_s < k \leq k_e \\ B, & k > k_e \end{cases} \quad (13)$$

where the values of C and α are chosen to ensure continuity. Four power spectrum parameters were varied in this model: the ratio of amplitudes before and after the break A/B with prior $[0.3, 7.2]$; k_s indicating the start of the break with prior $[0.01, 0.1]$ Mpc $^{-1}$; $\ln(k_e/k_s)$ to constrain the length of the break with prior $[0, 4]$ and normalisation A with prior $[14.9, 54.6] \times 10^{-8}$. We also placed a prior that k_e could not exceed 0.1 Mpc $^{-1}$.

Constraints on these parameters are shown in Fig. 4, in very good agreement with the Bridle et al. analysis showing that this parameterisation is robust in the extension to closed models. From the preference for a spectral index lower than unity in Sec 3.1 it is clear that a drop in power would be preferred by the data, especially if the transition was smooth and extended as this would mimic a tilted spectrum. Indeed this effect is seen by the large peak in the likelihood surface at very low values of $\ln(k_e/k_s)$ (i.e. a large difference in k_e and k_s implying an extended break). More interesting however is the preference for a sudden drop on large scales $k \approx 0.025$ Mpc $^{-1}$, this could be evidence for a phase transition in the early Universe, or as Bridle et al. point out, could be an artifact of the combination of WMAP and 2dF datasets. Example spectra featuring both extended and sharp breaks are shown in Fig. 5.

3.4 Power Spectrum Reconstruction

The data that can now be used to constrain the primordial power spectrum are generally analysed in the framework of a specific model, as we have done up to now. It is possible however that certain features of the observational data are being overlooked with this method. In order to reveal any

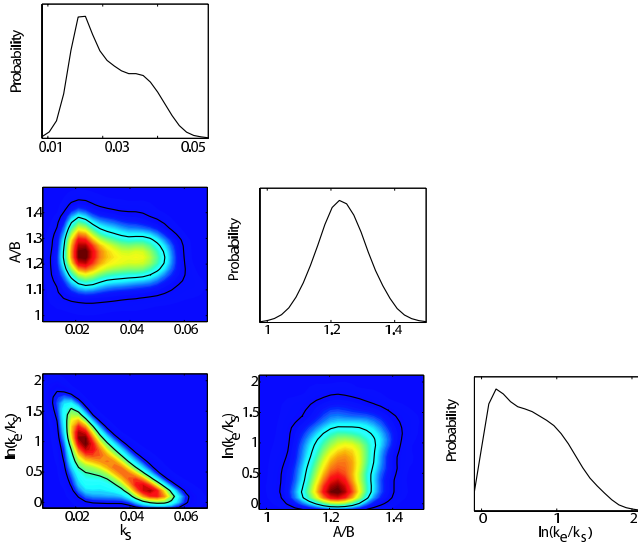


Figure 4. Marginalised 1D and 2D probability constraints on $k_s \ln(k_e/k_s)$ and A/B , 2D constraints plotted with 1σ and 2σ confidence contours.

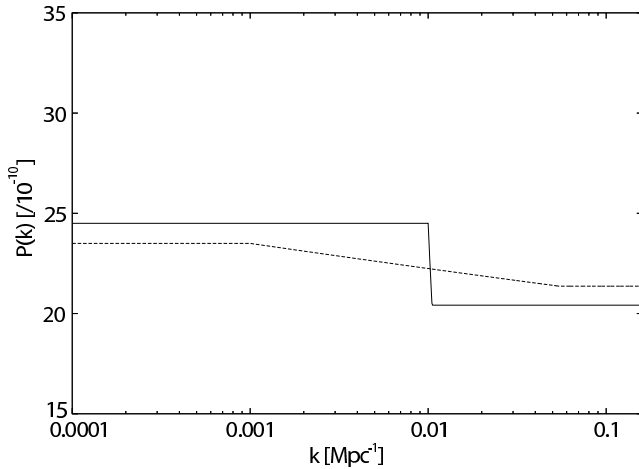


Figure 5. Examples of two broken spectra; with an extended and sudden transition in power.

such features we have divided the spectrum into eight bins in wavenumber k and allowed the amplitude in each bin to vary over the same range as the single amplitude A_s for the power law spectrum. Instead of using simple ‘tophat’ bin amplitudes we used the same approach as Bridle et. al, linearly interpolating between the bins in k . Since current interest has concentrated on large scale departures from scale invariance we confined the study to bins, of amplitude a_n , between 0.0001 and 0.11 Mpc^{-1} parameterised logarithmically with $k_{i+1} = 2.75k_i$ so that

$$P(k) = \begin{cases} \frac{(k_{i+1}-k)a_i + (k-k_i)a_{i+1}}{k_{i+1}-k_i}, & k_i < k < k_{i+1} \\ a_n, & k \geq k_n \end{cases} \quad (14)$$

We show in Fig. 6 the reconstructed spectrum relative to the best fit Harrison-Zel'dovich (H-Z). The effect of degeneracies between neighbouring bins is minimised with the use of *cosmoMC*'s new parameterisation to explore the $A_s - \tau$ degeneracy, however there is still considerable variability at

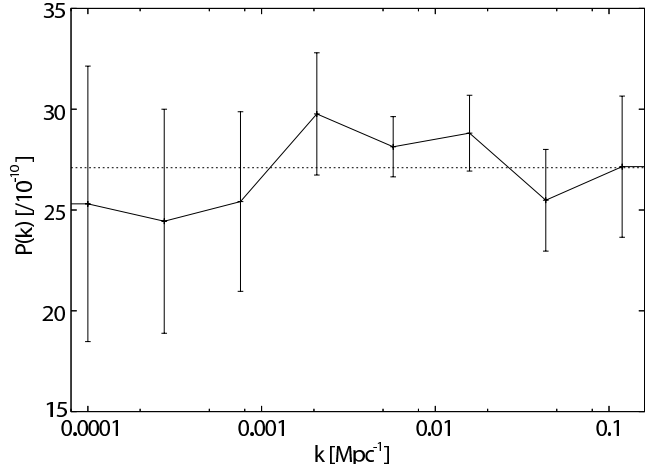


Figure 6. Reconstruction of the primordial power spectrum in 8 bands of k , compared to the best fit H-Z spectrum (dotted line).

the 1σ level. Our results are mostly in agreement with a H-Z spectrum, although we also find the feature observed at around 0.06 Mpc^{-1} by Bridle et al. We observe a slight decrement in the power on scales below 0.001 Mpc^{-1} , confirming results by Hannestad (2004), this effect would produce a similar decrement in the CMB spectrum at low l .

3.5 Closed Universe Inflation

Lasenby & Doran (2005) arrived at a novel model spectrum by considering a boundary condition that restricts the total conformal time available in the Universe, and requires a closed geometry. The resultant predicted perturbation spectrum encouragingly contains an exponential cutoff (as previously suggested phenomenologically by Efstathiou (2003a)) at low k which yields a corresponding deficit in power in the CMB power spectrum. The shape of the derived spectrum was parameterised by the function:

$$P(k) = A(1 - 0.023y)^2(1 - \exp(-(y + 0.93)/0.47))^2, \quad (15)$$

$$\text{where } y = \ln\left(\frac{k}{H_0/100} \times 3 \times 10^3\right) > -0.93.$$

Unfortunately it has not been possible to produce a routine that can recalculate the form of this spectrum (see Fig. 7) in non-primordial parameter space fast enough to perform a full MCMC analysis. The authors did, however suggest a best-fit cosmology ($\Omega_b h^2 = 0.0224$, $\Omega_{cdm} h^2 = 0.110$, $h = 0.6$ and a total energy density $\Omega_0 = 1.04$) from which we could fit the primordial spectrum using just an amplitude A with prior $[14.9, 54.6] \times 10^{-8}$. Although such a low Hubble parameter would have been ruled out from previous analyses (Spergel et al. 2003) the extension to non-flat geometries weakens the constraint considerably, as discussed earlier. The best fitting spectrum ($A = 29.82 \pm 0.19$) is shown with the H-Z, single index, cutoff and running index models for comparison in Fig 7. Encouragingly the ‘turn-over’ scale of the L+D spectrum is close to that found in the reconstructed spectrum at about 0.001 Mpc^{-1} , while at large k the spectrum successfully mimics a power law spectrum with spectral index $n_s \approx 0.96$.

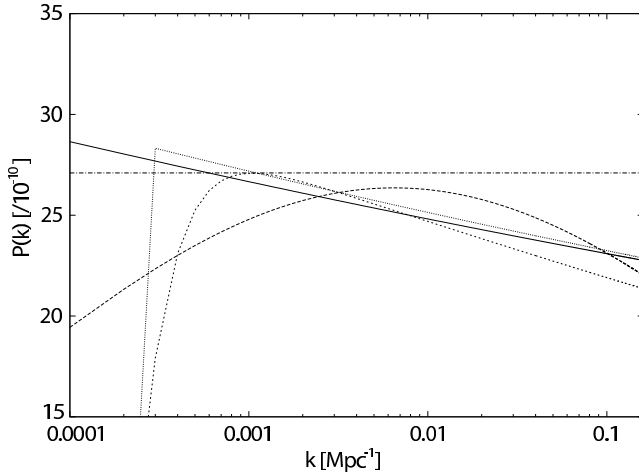


Figure 7. Lasenby & Doran spectrum (short-dashed) shown with best fitting H-Z (dot-dashed), single index with a cutoff (dotted), without (full) and a running index (long-dashed).

4 APPLICATION TO SIMULATED DATA

In order to test the model selection algorithm we produced a series of simulated data sets with known cosmological parameters and a particular primordial power spectrum parameterisation. We produced two sets: the first intended to represent the quality expected from the forthcoming Planck satellite mission, the second a combination of simulated WMAP first year CMB data and Sloan Digital Sky Survey (SDSS) large scale structure data. At least eight separate Markov chains were produced giving eight estimates of the evidence and an associated variance. The chosen model was flat with $\Omega_b h^2 = 0.022$, $\Omega_{cdm} h^2 = 0.120$, $h = 0.72$, optical depth to re ionisation of $\tau = 0.15$ and with primordial parameters $n_s = 0.97$ and $A_s = 2.5 \times 10^{-9}$.

4.1 Simulated Planck Data

We approximated mock Planck data as being cosmic variance limited up to l of 2000, which was sufficiently accurate to determine the spectral index n_s in such a parameterisation to an accuracy of better than 2% and was produced using C_l s from the power spectrum generator *CAMB* (Lewis, Challinor & Lasenby (2000)) to which we added Gaussian noise with a cosmic variance standard deviation of

$$\Delta C_l^2 = \frac{2}{l(l+1)} C_l^2 \quad (16)$$

The CMB spectrum of the chosen model is shown in Fig. 8 along with the data points used including simulated noise. Parameter constraints confirm that the sampler is capable of extracting this model from the dataset (see Fig. 9).

Since the absolute evidence value can only be compared between models using the same dataset it is conventional to quote ratios with respect to a reference model, which in this case will be the single spectral index. Our results (shown in Table 2) successfully select the correct model, although with high variance between chains. In particular, the cutoff model is, within estimated 1σ error, a very close second. This is not too surprising given that the cutoff spectrum is simply

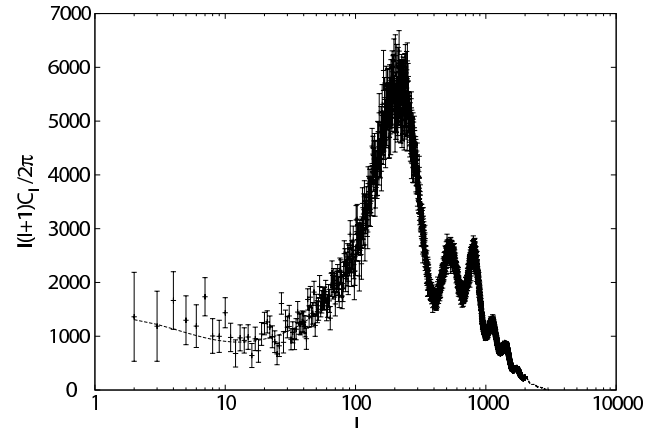


Figure 8. Simulated cosmic variance limited data to $l = 2000$ (convolved with Gaussian noise) and the model from which it was produced (dashed line).

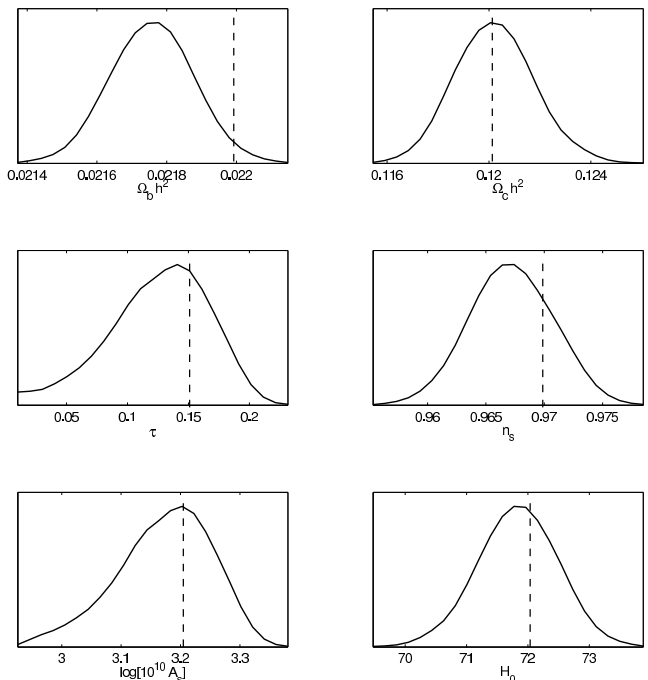


Figure 9. Recovered MCMC marginalised parameter constraints using cosmic variance limited data.

Table 2. Differences of log evidences for four parameterisations using cosmic variance limited data.

Model	$\ln E_\Lambda - \ln E$
Constant n	0.0 ± 2.4
Running	-4.7 ± 2.2
Cutoff	-1.1 ± 2.9
Broken	-36.7 ± 3.3

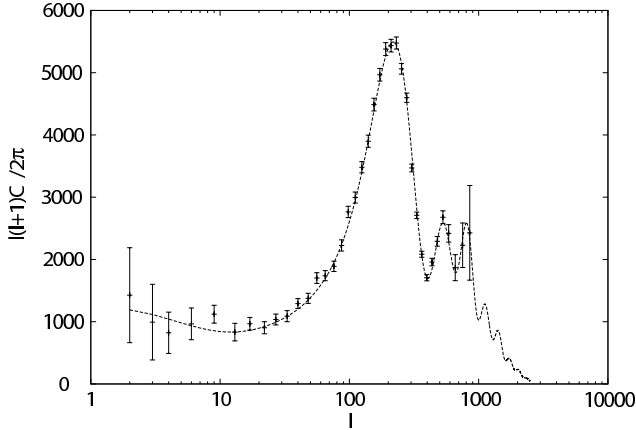


Figure 10. Simulated first year WMAP data to $l = 856$ and the model from which it was produced (dashed line).

a single index spectrum above the appropriate cutoff wave vector k_c , at which scale cosmic variance is large enough to prevent one obtaining strong constraints. The question of what difference in log evidence one requires to say with some certainty which model the data prefers is not a trivial one and depends to some extend on ‘intuition’. A useful guide has been given by Jeffreys (1961) where a log evidence difference: $\Delta \ln E < 1$ is not significant, $1 < \Delta \ln E < 2.5$ significant, $2.5 < \Delta \ln E < 5$ strong and $\Delta \ln E > 5$ decisive. Using this criterion we can correctly rule out, with some confidence, the running index spectrum and completely discount the broken model. The combination of some large scale structure data sets would doubtless allow a distinction between the cutoff and single index spectrum though this test has not, as yet been performed.

4.2 Simulated WMAP & SDSS Data

Two further datasets were created to mimic the current data used in our full analysis: a simulated first year WMAP CMB power spectrum and large scale structure data similar to the SDSS matter power spectrum. Both spectra were again produced using the *CAMB* generator using the same single index model chosen above. The mock WMAP C_l s were created by adding Gaussian noise using the calculated WMAP errors at multipoles between 2 and 856 corresponding to the binning used by the WMAP team (see Fig. 10). SDSS data was produced (see Fig. 11) using the binning in k space and calculated errors used by (Abazajian et al. 2003). As is well known the combination of LSS and CMB data is capable of breaking a number of degeneracies in parameter space and can produce tighter constraints than with CMB data alone (see Fig. 12). Although differences in the evidence estimates made with this realistic data are somewhat smaller than with simulated Planck data it is still possible to determine the correct model, though not decisively (Table 3) according to Jeffreys criteria.

5 APPLICATION TO REAL DATA

Given the success of model recovery using simulated data, we can now turn back to real data with some confidence. All

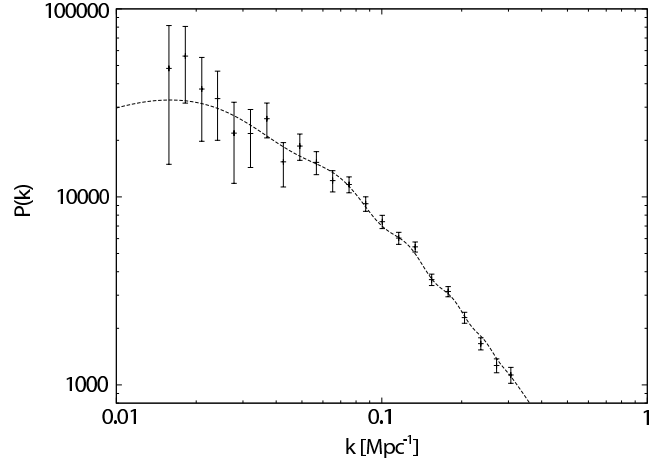


Figure 11. Simulated SDSS data and the matter power spectrum from which it was produced (dashed line)

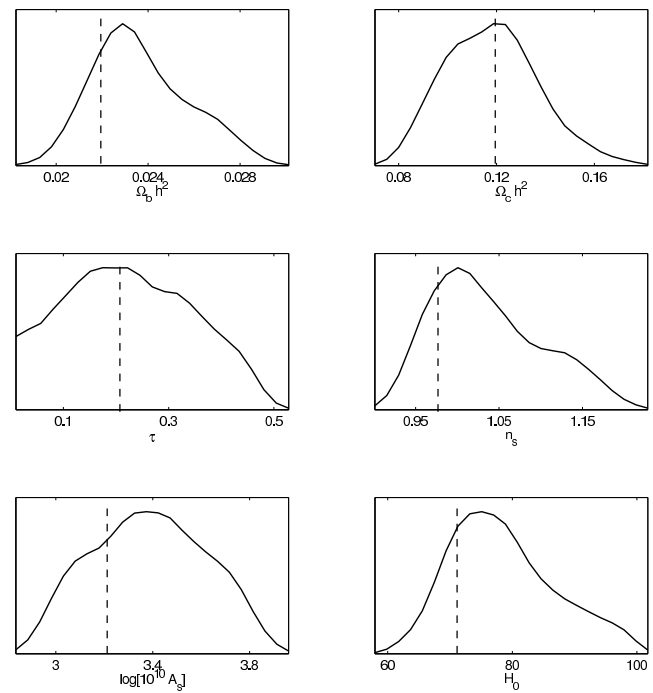


Figure 12. Recovered MCMC marginalised parameter constraints for the chosen model using simulated first year WMAP + SDSS data.

Table 3. Differences of log evidences of four models using a combination of simulated WMAP and SDSS data.

Model	$\ln E_A - \ln E$
Constant n	0.0 ± 0.8
Running	-2.3 ± 0.8
Cutoff	-1.2 ± 0.6
Broken	-1.1 ± 1.5

of the parameter estimations in Sec. 3 were accompanied by at least eight separate log evidence estimates. We can divide this part of the analysis into two main sections: firstly a full parameter space exploration for the H-Z, single index, running, cutoff, broken and binned models; and secondly estimations made only with the reduced primordial parameter space (i.e. only those parameters affecting the form of the initial power spectrum) within a predetermined cosmology, to include the Lasenby & Doran model. This division was necessary because of the restrictions in the form of the Lasenby & Doran spectrum discussed in Sec. 3.5.

5.1 Full cosmological parameter space exploration

Statistical uncertainty dominates the results of the full parameter space study (see Table 4), leaving it difficult to draw any meaningful conclusions. All of the central mean values, with the exception of the binned spectrum, are found to differ by less than a unit in log evidence, which, according to Jeffreys criteria, provides an insignificant difference in evidences. However ranking these mean values we find that the cutoff spectrum is marginally preferred overall. Although a better chi-squared fit was found by Spergel et al. (2003) for a running parameterisation we find no conclusive evidence in its favour in this study. Indeed it is worth noting, any possible preference for a typical running spectrum ($n_{run} \approx -0.035$) could possibly be due to its large scale power decrement rather than any running. The reconstructed spectrum, revealing any possible structure would be expected to provide the best possible model fit –however the large increase in parameter space has clearly had a detrimental effect producing a ‘significant’ evidence result disfavouring the model. In order to reduce the statistical uncertainty in these estimates to the point of distinguishing between the best fit models we would require of order 50 separate runs for each parameterisation which at present is not computationally feasible. However the use of the alternative method of nested sampling (see Mukherjee, Parkinson & Liddle (2005)) could allow the reduction of uncertainties to the required level in a future study.

5.2 Primordial parameter space exploration

The Lasenby & Doran spectrum had previously been calculated for a cosmological model described by $\Omega_0 = 1.04$, $\Omega_b h^2 = 0.0224$, $h = 0.6$, $\Omega_{cdm} h^2 = 0.110$, and provided a good fit to WMAP and higher resolution data. We therefore used this cosmology as a starting point. Again the results (see Table 5) have been normalised to the single index spectrum, and the similarity in evidences make it difficult to distinguish between the H-Z, single index and cutoff. We can however clearly rule out the running spectrum in this case with some certainty. Though not a convincing result in this case, the mean evidence of the Lasenby & Doran spectrum lies slightly higher, quantitatively confirming the ‘hand’ fit used in Lasenby & Doran (2005).

With this relative success for a restricted cosmology, it made sense to consider the evidence rankings within the best fit concordance cosmology, in this case the parameter estimates found from the full MCMC simulations of the power spectrum. A general package for predicting

Table 4. Differences of log evidences with respect to single index model using the full cosmological parameter space.

Model	$\ln E_\Lambda - \ln E$
Constant n	0.0 ± 0.7
H-Z	0.4 ± 0.8
Running	0.5 ± 0.7
Cutoff	0.8 ± 0.8
Broken	-0.3 ± 0.8
Binned	-1.8 ± 0.7

Table 5. Differences of log evidences (for primordial parameters) for all models with respect to single index model within cosmology: $\Omega_0 = 1.04$, $\Omega_b h^2 = 0.0224$, $H_0 = 60$, $\Omega_{cdm} h^2 = 0.110$.

Model	$\ln E_\Lambda - \ln E$
Constant n	0.0 ± 0.6
H-Z	-0.4 ± 0.5
Running	-2.1 ± 0.5
Cutoff	0.2 ± 0.6
Broken	-0.5 ± 0.7
Binned	-5.2 ± 0.7
Lasenby & Doran	0.9 ± 0.6

the power spectrum for arbitrary parameters within the Lasenby & Doran model is not currently available, however we know the form to be fairly stable with varying cosmological parameters. Hence we used the $\Omega_0 = 1.04$ model described above as a template to compare with the results from the full MCMC fitting, which gave parameters $\Omega_0 = 1.024$, $\Omega_b h^2 = 0.0229$, $h = 0.61$, $\Omega_{cdm} h^2 = 0.118$. Although these correspond to a different cosmology from that used for the Lasenby & Doran case, the cosmological parameters do not deviate greatly from these across the different parameterisations, in particular the cutoff and running cases, hence we feel an evidence comparison is justified. This result (Table 6), shows the L+D model to lie roughly 3 units of log evidence ahead of the cutoff case, yielding an evidence ratio of roughly 20, which according to the Jeffreys ranking system provides a ‘strong’ model selection.

Table 6. Differences of log evidences (for primordial parameters) for all models with respect to single index model within the current concordance cosmology: $\Omega_0 = 1.024$, $\Omega_b h^2 = 0.0229$, $h = 0.61$, $\Omega_{cdm} h^2 = 0.118$, as compared to the Lasenby & Doran model (with parameters as in the previous table)

Model	$\ln E_\Lambda - \ln E$
Constant n	0.0 ± 0.5
H-Z	-4.4 ± 0.5
Running	-0.8 ± 0.6
Cutoff	0.4 ± 0.5
Broken	-2.7 ± 0.6
Binned	-6.1 ± 0.6
Lasenby & Doran	4.1 ± 0.5

6 CONCLUSIONS

We have performed a full Bayesian analysis of various parameterisations of the primordial power spectrum which includes not only the estimation of cosmological and spectral parameters but also a value of the Bayesian evidence. This method of model selection was tested using simulated current and future data, though it is difficult to make conclusive determinations in most cases using real data at present. Consistently high evidence values were obtained for those models incorporating a reduction in power at low k , a natural result given the 1st year WMAP data. In particular we found strong evidence in favour of the Lasenby & Doran spectrum within a limited MCMC analysis.

ACKNOWLEDGEMENTS

We acknowledge A. Slosar for permission to use his Bayesian evidence code, S. Bridle, A. Lewis and A. Liddle for useful discussions. This work was carried out largely on the COSMOS UK National Cosmology Supercomputer at DAMTP, Cambridge and we would like to thank S. Rankin and V. Treviso for their computational assistance. MB was supported by a Benefactors Scholarship at St. John's College, Cambridge and an Isaac Newton Studentship.

REFERENCES

Abazajian K., Adelman-McCarthy J. K., Agueros M. A., Allam S. S., Anderson S. F., Annis J., Bahcall N. A., Baldry I. K., et al., 2003, ApJ, 126, 2081

Adams J.A., Ross G.G. & Sarkar S., 1997, Nucl. Phys. B. 503, 405

Barriga J., Gaztanaga E., Santos M.G., Sarkar S. 2001, MNRAS, 324, 977

Beltran M., Garcia-Bellido J., Lesgourgues J., Liddle A., Slosar A., 2005, Phys. Rev. D, 71, 063532

Bridle S., Lewis A., Weller J., Efstathiou G., 2003, MNRAS, 342, L72

Dickinson C. et al., 2004, MNRAS, 353, 732

Dodelson S., Stewart E., 2002, Phys. Rev. D. 65, 101301

Efstathiou G., 2003, MNRAS, 346, 26

Efstathiou G., 2003, MNRAS, 343 L95

Guth A., 1981, Phys. Rev. D, 23, 347

Hannestad S. J. Cosmol. Astropart. Phys., 2004, JCAP 04(2004)002

Hinshaw G. et al. Astrophys. J. Suppl., 2003, 148, 135

Hobson M.P., McLachlan C., 2003, MNRAS, 338, 765

Jeffreys H., 1961, *Theory of Probability*, 3rd ed., Oxford University Press

Kogut A. et al., 2003, Astrophys. J. Suppl., 148, 161

Kuo C.L. et al., 2004, Ap. J., 600, 32

Lasenby A.N, Doran, C., 2005, Phys.Rev. D 71, 063502

Lewis A. and Bridle S., 2002, Phys. Rev. D, 66, 103511

Lewis A., Challinor A., Lasenby A., 2000, ApJ, 538, 473

Linde A.D., 1983, Phys. Rev. Lett. B, 129, 177

Lyth D.H., Riotto A., 1999, Phys.Rept. 314 1-146

Mukherjee, P. Parkinson D. Liddle, A., 2005, astro-ph/0508461

Mukherjee P. & Wang Y., 2003, Astrophys. J., 593, 38

Niarchou A., Jaffe A., Pogosian L., 2004, Phys.Rev. D 69 063515

Percival W.J. et al., 2001, MNRAS, 327, 1297

Readhead A.C.S. et al., 2004, ApJ, 609, 498–512

Rebolo R. et al., 2004, MNRAS, 353, 747

Slosar A. and Hobson M.P., 2003, astro-ph/0307219

Slosar A. et al., 2003, MNRAS, 341, L29

Spergel D.N. et al., 2003, Astrophys. J. Suppl., 148, 175

Tocchini-Valentini D., Douspis M., Silk J., 2005, MNRAS 359

Trotta R., 2005, astro-ph/0504022

Wang Y., 1994, Phys. Rev. D, 50, 6135

Verde L. et al., 2003, Astrophys. J. Suppl., 148, 195